Viscoelastic model for analysing the behaviour of adhesive-bonded FRP-to-steel joints in civil engineering applications

Citation for published version:
Wang, S, Stratford, T & Reynolds, TPS 2023, 'Viscoelastic model for analysing the behaviour of adhesive-bonded FRP-to-steel joints in civil engineering applications', *International journal of adhesion and adhesives*, vol. 123, 103359. https://doi.org/10.1016/j.ijadhadh.2023.103359

Digital Object Identifier (DOI):
10.1016/j.ijadhadh.2023.103359

Published In:
International journal of adhesion and adhesives

Viscoelastic model for analysing the behaviour of adhesive-bonded FRP-to-steel joints in civil engineering applications

S. Wang[a,b,*], T. Stratford[c] and T.P.S Reynolds[c]

[a] School of Civil Engineering, Architecture and Environment, Hubei University of Technology, Wuhan 430068, China
[b] Innovation Demonstration Base of Ecological Environment Geotechnical and Ecological Restoration of Rivers and Lakes, Hubei University of Technology, Wuhan 430068, China
[c] School of Engineering, Institute for Infrastructure and Environment, The University of Edinburgh, Edinburgh EH9 3FG, UK

Email: wangsongbo@hbut.edu.cn, tim.stratford@ed.ac.uk, t.reynolds@ed.ac.uk
* Corresponding Author

Abstract

Adhesively bonding fibre reinforced polymer (FRP) plates have been a mainstream method for strengthening civil engineering structures. The effectiveness of bonding strengthening is dependent on the performance of the adhesive layer. This study examines the time-temperature dependent viscoelasticity of a typical structural epoxy adhesive and develops a linear viscoelastic material model that can be used for numerical analysis. An accelerated test method involving dynamic mechanical analysis (DMA) and time-temperature superposition principle (TTSP) were used to characterise the structural adhesive. The corresponding limitations of this method were discussed, including decomposition effect, nonlinear viscoelasticity, applicability of TTSP, and further curing of the sample. The numerical study of the long-term behaviour of the single lap-shear FRP-to-steel joint found that a slightly warmer temperature (30 °C for this study) is beneficial for the bonded joint as it can reduce the concentrated shear stress with negligible increase in the shear strain. However, a higher temperature (50 °C for this study) that near the adhesive's glass transition temperature (T_g) could be detrimental as it can lead to significant shear strain in the adhesive joint within the first year of service life.

Keywords: Structural epoxy adhesive; Viscoelasticity; Elevated temperature; DMA; FRP-to-steel joint.

1 Introduction

Adhesives have been widely used in various industries including automotive, aircraft, and aerospace, since their advent [1–3]. Also for civil engineering, with the rapidly growing need of rehabilitating and strengthening existing structures, adhesively bonding an FRP plate has currently been a mainstream strengthening method [4–6]. Compared to traditional strengthening methods involve welding, bolting, or riveting, the use of adhesively bonding can bring advantages such as lower additional weight, lower time and labour intensity, and more uniformly distributed stresses in the bonding area [7–13].

The effectiveness and reliability of bonding strengthening are significantly dependent on the quality, integrity, and durability of the adhesive layer which acts as a load transfer medium between the composite and structure. Especially for FRP-to-steel joints, the adhesive layer inevitably becomes the weakest section due to its relatively lower strength and stiffness [3,14–16]. Commonly used ambient-cured adhesives are typically made of viscoelastic polymers. Thermal exposure can soften the adhesive and induce temperature- and time- dependent viscoelastic creep along bonded joints, which may be detrimental and hence affect the performance of strengthened structures [17–22]. In current design guidelines for strengthening civil engineering metallic structures using FRP, this issue is avoided by simply limiting the maximum operating temperature to a minimum of 15 °C below the peak Tan δ glass transition temperature (T_g) of the bonding adhesive and using a multiple combination of large safety factors, which reduces the design efficiency and hampers the extensive use of this advanced strengthening method [7,10,23–25]. A more profound understanding of how the time-temperature related viscoelasticity of adhesives affects the performance of bonded joints is desired.

1.1 Literature survey

The existing studies on FRP-to-steel bonded joints in structures have been mainly focusing on their short-term performance [18,20,26,27]. While Heshmati *et al.* [5] examined the performance of FRP-to-steel double lap-shear joints after immersed in distilled water at 20 °C and 45 °C for up to three years and found that there was a noticeable greater strength reduction in those joints immersed at 45 °C. De Zeeuw *et al.* [19] investigated the effects of 40 °C air (or distilled water) and constant load on the behaviour of single lap-shear joints. Within 14 days of sustained loading test, they observed the time-dependent viscoelastic creep behaviour. However, the design service life of civil engineering constructions is more than decades. The results obtained by these conventional experimental methods are usually limited.

Another research strategy is to use an accelerated test method to directly characterise the viscoelasticity of adhesives, as it is the major factor responsible for the deterioration of joints' performance. Dynamical mechanical analysis (DMA) is a common technique used to characterise the viscoelasticity of polymers as a function of temperature and frequency (or time). The time-temperature superposition principle (TTSP) is classically applied along with the DMA test, which allows the viscoelastic behaviour at a lower frequency (or over a longer time) to be estimated from the behaviour at a higher frequency (or over a shorter time), but at another higher temperature, thus avoiding the limitations of the measurement instruments [16,28–30]. This method has been used in several studies in other industries [16,21,29,30], however, relevant studies in civil engineering are limited, and the data and conclusions from other studies may not be applicable due to differences in types of adhesives, curing conditions, operating temperatures, and useful service life [3].

Houhou *et al.* [25] examined the viscoelasticity of a structural epoxy adhesive using aforementioned accelerated test method (DMA and TTSP), but the further analysis was conducted on the behaviour of FRP-to-concrete joints, in which concrete might be the weakest part. Nevertheless, the study found that the viscoelastic creep can induce a redistribution of interfacial stresses, leading to a reduction in the concentrated peak stress and an increase in effective transfer length, which could be beneficial for the durability of bonded joints. However, this work did not further consider the temperature effect on the joint, which may bring greater creep deformation. The authors [31] previously examined a strengthening adhesive with a relatively low onset T_g (38.0 °C) for investigating the worst case of viscoelastic creep at elevated temperatures. Whilst it was found that the creep reduced the performance of FRP-strengthened metallic beams during the long-term services, the details of stress redistribution and increased strain within the bonded joints were not shown, and the authors were also aware that the characteristic data of the adhesive with low T_g may be less representative. Besides, none of these studies discussed the limitations of using the accelerated test method, leaving it unclear whether the structural adhesive decomposed during the DMA test at high temperatures, and whether applying the TTSP was feasible without introducing substantial errors.

Against this background, the objectives of this study are (a) charactering the viscoelasticity of a typical structural adhesive; (b) discussing the limitations of the applied accelerated test method and identifying the need for further research; (c) obtaining a profound understanding of the impact of elevated temperatures on the long-term behaviour of FRP-to-steel joints.

2 Experimental characterisation of viscoelasticity

The structural adhesive characterised in the present study was a two-component epoxy resin, Sikadur®-330 [32], which has been widely used in FRP strengthening for civil engineering structures. The adhesive samples used in these tests were cured at ambient temperature (21 ±

2 °C) and humidity (50 ± 10% RH) for 28 days, which could be consistent with the practical strengthening application and ensured that the samples had reasonable T_g values. Prior to characterising the viscoelasticity of the adhesive through DMA tests at high temperatures, the thermogravimetric analysis (TGA) test was conducted to characterise its thermal stability in order to determine the maximum applicable experimental temperature. Combining the DMA test with TTSP, a complete modulus master curve was then constructed. The usage range of applying TTSP was also discussed.

2.1 Thermogravimetric analysis (TGA)

In many studies that apply DMA to conduct the accelerated characterisation of adhesives at high temperatures (> 100 °C), the thermal stability of the tested sample was not examined [16,30,31]. However, when the temperature rises above 100 °C, the loss of mass attributed to the evaporation of low molecules from epoxy adhesives may have started, as structural epoxy adhesives typically contain fillers, curing agents, and accelerators [32–35]. This can therefore affect the obtained modulus response data and thus introduce errors.

In this study, the TGA experiment was conducted to examine the thermal stability of the studied adhesive according to ISO 11358 [36] through a Mettler Toledo thermogravimetric instrument. The powdery adhesive sample (15.1 mg) was placed in the aluminium oxide crucible which was set in the sample holder of the analyser. The test was run from 25 °C to 900 °C in an air atmosphere with a heating rate of 10 °C/min. Figure 1 shows the resultant mass loss curve and mass derivative curve.

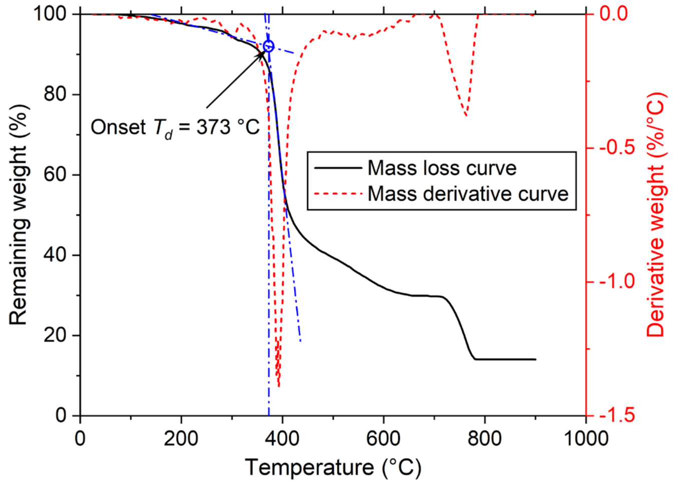

Figure 1: Decomposition temperature (T_d) of the adhesive

Whilst the obtained onset decomposition temperature (T_d) of the structural adhesive was 373 °C [36,37], the thermal decomposition behaviour started to occurs when the temperature exceeded approximately 100 °C. This suggests a maximum experimental temperature of 100 °C, below which the decomposition behaviour can be ignored.

2.2 Dynamic mechanical analysis (DMA)

The DMA characterising experiments were carried out according to ISO 6721 [38] through a DMA 8000 instrument. The dimensions of the rectangular adhesive specimen and applied configuration in each test are illustrated in Table 1.

Table 1: Dimensions of specimens and applied configurations in DMA tests

Test	Configuration	Dimension (mm)		
		Length	Width	Thickness
T_g	Single cantilever	35	7.45	1.59
Frequency scan		35	7.43	1.60
Strain scan	Dual cantilever	45	7.50	1.48

2.2.1 Glass transition temperature (T_g)

As mentioned in Section 1, the maximum working temperature of the structural bonded joint stipulated in the current design guidelines is based on the T_g of the applied adhesive [7,23]. T_g, as an important material property, indicates the transition temperature range of a thermoset polymer from a stiff glassy state to a rubbery state [39].

The DMA time/temperature scan test was carried out to determine the T_g of the examined adhesive, using a sinusoidal displacement of 0.05 mm at 1.0 Hz, and 2 °C/min temperature ramp [28,38]. The measured temperature-dependent storage modulus and Tan δ were shown in Figure 2.

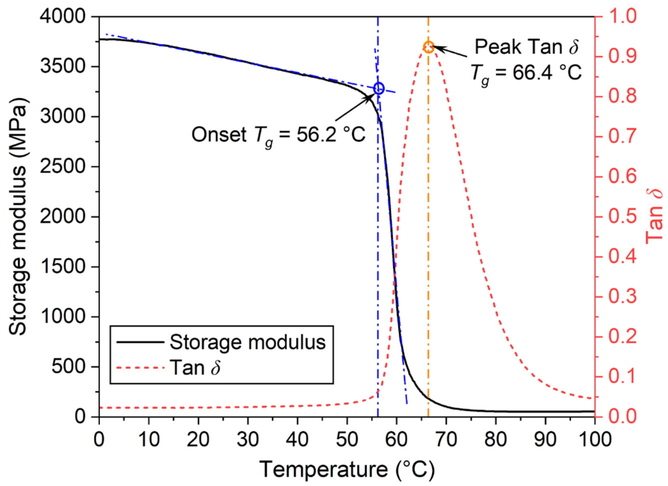

Figure 2: Glass transition temperature (T_g) of the adhesive

A significant reduction in the storage modulus occurred between the onset T_g (56.2 °C) and the peak Tan δ T_g (66.4 °C) [28,38]. In order to fully characterise the viscoelasticity of the adhesive at elevated temperatures, the average T_g (61.3 °C) was used as the benchmark intermediate temperature so that the applied temperature range of the subsequent viscoelastic characterising tests was set between 25 °C to 100 °C.

2.2.2 Modulus response in DMA strain scans

Strain scans measurements were performed by applying an oscillatory displacement of 1.0 Hz with amplitudes ranging from 0.006 mm to 0.100 mm, corresponding to applied strains of between approximately 0.012% and 0.197%, to examine whether the adhesive would exhibit nonlinear viscoelasticity. A dual cantilever configuration was utilised to guarantee that the sample was subjected to a generally uniform strain when large displacements were applied [28]. These scans were repeated at 5 °C intervals over a temperature range of 25 °C to 100 °C. Figure 3 illustrates the resultant storage modulus responses.

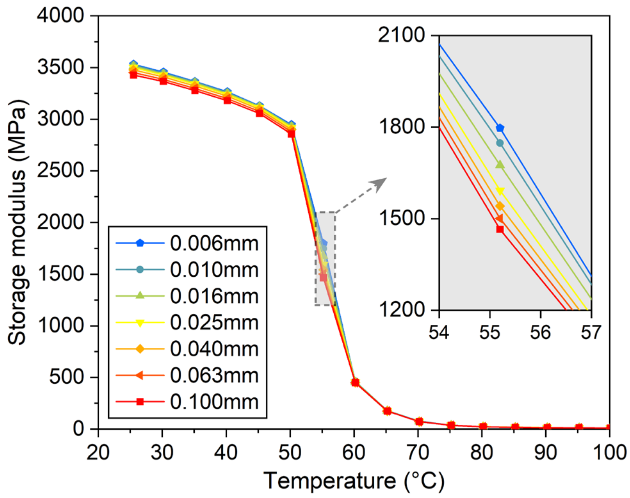

Figure 3: DMA multi-strain scans test

The examined adhesive exhibits very limited strain (stress) dependent behaviour. It is only when the temperature rises close to the T_g, resulting in a sharp drop in the storage modulus, that the behaviour of the adhesive shows a relatively noticeable nonlinearity. Consequently, in the current paper, the behaviour of the adhesive was discussed solely in terms of linear viscoelasticity.

Note that the strain (stress) applied in the DMA test is relatively minimal to prevent fatigue damage to the sample [28]. The adhesive may exhibit significant nonlinear viscoelastic behaviour when subjected to higher strain (stress). However, the stress redistribution behaviour of bonded joints at elevated temperatures can drastically reduce the stresses carried by the adhesive layer [25,27,40], and thus limit the effect of nonlinear response. Detailed investigation of the nonlinear viscoelasticity of adhesives was not, however, the focus of this paper.

2.2.3 Modulus response in DMA frequency scans

The viscoelastic response of the structural adhesive was examined using DMA multi-frequency scans test [28]. The specimen was exposed to a sinusoidal displacement of 0.01 mm at frequencies ranging from 0.01 Hz to 100 Hz, logarithmically spaced to cover five measurements pre decade. The test was carried out over a temperature range of 25 °C to 100 °C with a temperature step of 5 °C. The obtained storage modulus that increased with frequency but decreased with temperature is shown in Figure 4 (a), and the corresponding loss modulus is shown in Figure 4 (b).

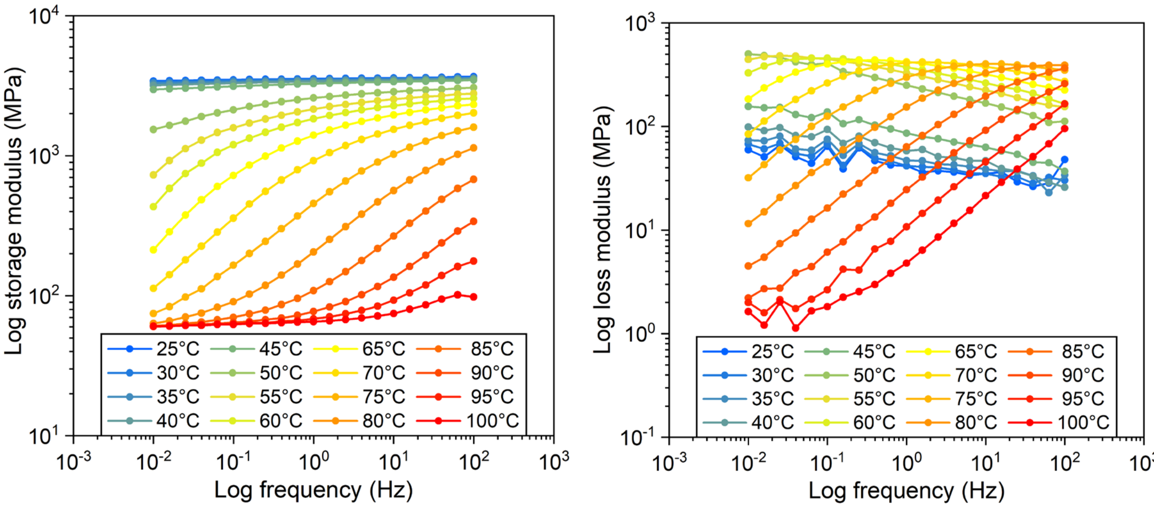

(a) storage modulus variation (b) loss modulus variation

Figure 4: DMA multi-frequency scans test

2.2.4 Time-temperature superposition principle

As mentioned in the literature review, TTSP has been used in a number of studies to build modulus master curves of adhesives based on DMA viscoelastic characterisation results [16,21,25,29–31]. However, most of studies did not consider the applicability of TTSP, which raised concerns about the accuracy of developed master curves.

TTSP is applicable to thermorheologically simple materials whose viscoelastic response depend equally on temperature [41,42]. The wicket plot (log Tan δ versus log storage modulus) is one way to identify the thermorheologically simplicity of materials [28,29,41]. Based on the results of the DMA multi-frequency scans test (Figure 4), the wicket plot for the adhesive investigated in this study is shown in Figure 5. The near-arch shape (near symmetrical curve) indicates the thermorheologically simplicity, so as to confirm the applicability of TTSP [28,29,41].

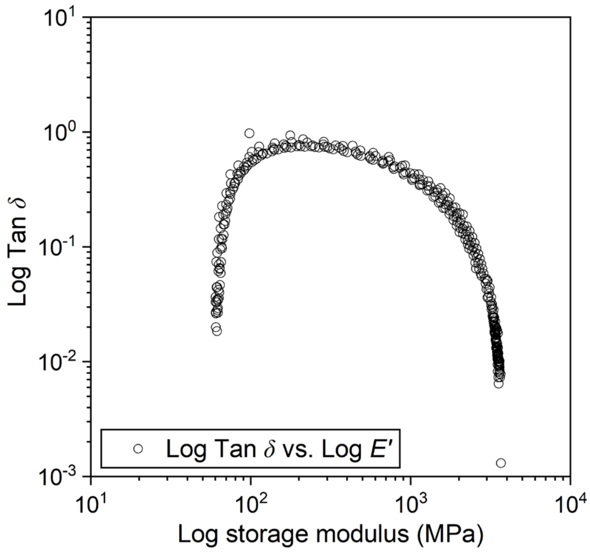

Figure 5: Wicket plot for the examined Sikadur®-330

According to TTSP, as shown in Figure 6, the horizontal shift was applied to the individual measurements (Figure 4) to form the master curve at the reference temperature of 55 °C (Figure 6 (b)), which is the closest temperature step to the adhesive's onset T_g, where the modulus begins to drop significantly. The determined shift factors (α_T) are fitted to the well-known Williams-Landel-Ferry (WLF) equation (Figure 6 (c)) [28,30]:

$$log(\alpha_T) = \frac{-C_1(T - T_{ref})}{C_2 + (T - T_{ref})} \quad (1)$$

where T is the temperature of interest, C_1 = 30.48 and C_2 = 151.14 (°C) are obtained calibration constants. The corresponding shifted loss modulus using the same shift factors are illustrated in Figure 6 (d), showing a good continuity as well.

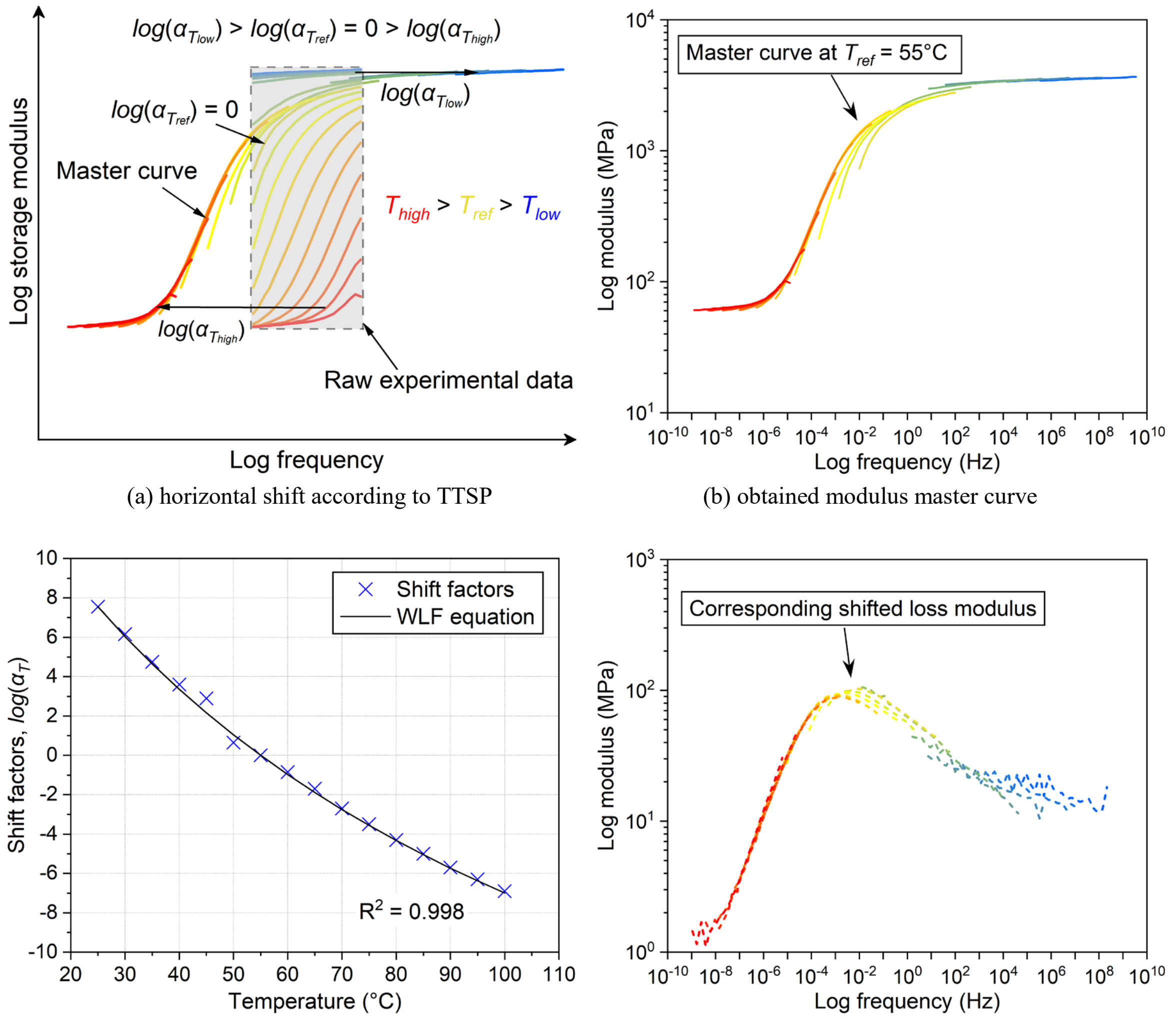

(a) horizontal shift according to TTSP

(b) obtained modulus master curve

(c) shifted factors fitted to WLF equation

(d) corresponding shifted loss modulus

Figure 6: Master curve at T_{ref} = 55°C obtained using TTSP

3 Material modelling

3.1 Calibration of the linear viscoelastic material model

A Prony series, expressing the generalised Maxwell model, was used for the linear viscoelastic model, which is an in-built material model in the Abaqus analysis software. The shifted storage modulus and loss modulus shown in Figure 6 were fitted to a Prony series in the frequency domain [43,44]:

$$E'(\omega) = E_0\left(1 - \sum_{i=1}^{n} e_i\right) + E_0 \sum_{i=1}^{n} \frac{\omega^2 {\tau_i}^2 e_i}{\omega^2 \tau_i^2 + 1} \tag{2}$$

$$E''(\omega) = E_0 \sum_{i=1}^{n} \frac{\omega \tau_i e_i}{\omega^2 {\tau_i}^2 + 1} \quad (3)$$

where E_0 is the instantons elastic modulus, $E'(\omega)$ is the storage modulus, $E''(\omega)$ is the loss modulus, ω is the angular frequency, and i presents the number of terms in Prony series. τ_i and e_i are the parameters indicating the relaxation times and relaxation modulus respectively. In addition, in the Abaqus, a Prony series in time domain using the same parameters can be used to calculate the time-dependent modulus response [43,44]:

$$E(t) = E_0 \left[1 - \sum_{i=1}^{n} e_i \left(1 - e^{-t/\tau_i}\right) \right] \quad (4)$$

The fitting results are illustrated in Figure 7 and the obtained parameters are presented in Table 2. In general, the fitting is satisfactory, and it is typical for the Prony series that the fitting to the storage modulus is more accurate than the fitting to the loss modulus [16,28,42]. However, in many studies, the fitting to the loss modulus is ignored or not shown [21,25,30,31], which makes the accuracy of fitting unclear.

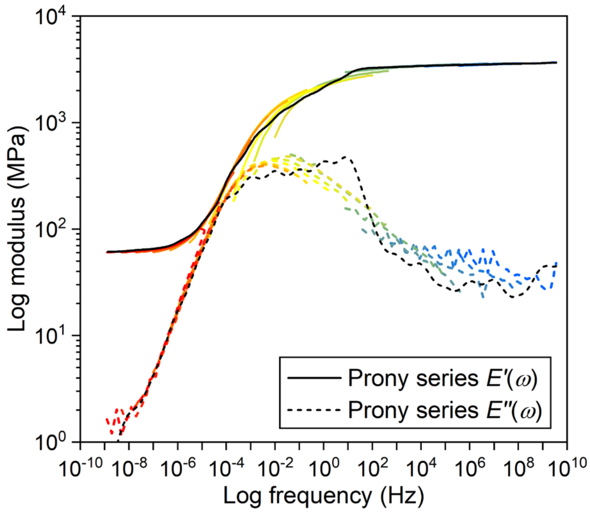

Figure 7: Comparison of Prony series fitting versus shifted experimental values

Table 2: Parameters of the obtained viscoelastic material model

Prony series			
τ_i (s)	e_i	τ_i (s)	e_i
1×10^{-10}	0.0224	1×10^{1}	0.1295

1×10^{-9}	0.0180	1×10^{2}	0.1333
1×10^{-8}	0.0057	1×10^{3}	0.1213
1×10^{-7}	0.0137	1×10^{4}	0.0724
1×10^{-6}	0.0124	1×10^{5}	0.0147
1×10^{-5}	0.0084	1×10^{6}	0.0043
1×10^{-4}	0.0186	1×10^{7}	0.0008
1×10^{-3}	0.0196	1×10^{8}	0.0007
1×10^{-2}	0.0136	$\sum e_i = 0.9836$	
1×10^{-1}	0.2141	$E_0 = 3730$ MPa; $\mu_0 = 0.45$	
1×10^{0}	0.1601	$k_i = 0$	
WLF equation			
$T_{ref} = 55$ °C	$C_1 = 30.48$	$C_2 = 151.14$ (°C)	

For simplicity, the bulk modulus (k_i) and Poisson's ratio (μ_0) of the adhesive are considered to be independent of time (Table 2), which is usually acceptable for polymers [16,43,44]. In Section 4, the above parameters are applied into the Abaqus FE software to analyse the joint creep behaviour caused by the thermal-viscoelastic response of the adhesive layer. The viscoelasticity of the adhesive is defined by entering each term of the Prony series (τ_i, e_i, and k_i) through the Abaqus *material-viscoelastic* option, while the temperature dependence is defined through the sub-option, *Trs*, using the WLF equation parameters (T_{ref}, C_1, and C_2).

3.2 Accuracy investigation of the obtained material model

Figure 8 illustrates a comparison between the predicted values of the viscoelastic material model (Prony series) and the original experimental values illustrated in Section 2.2.

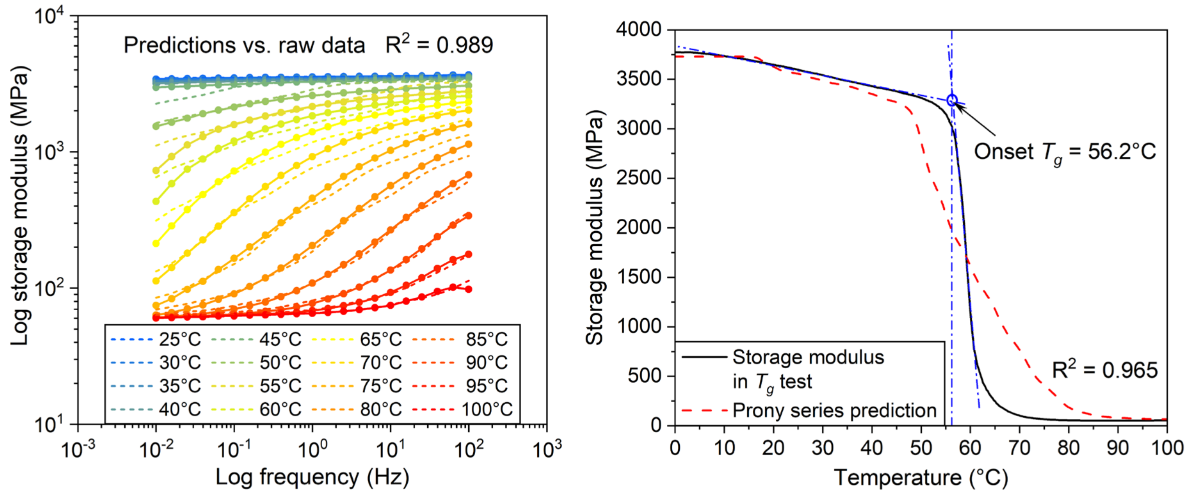

(a) compared to DMA multi-frequency scans test results (b) compared to DMA T_g test results

Figure 8: Comparison of viscoelastic model predictions versus raw experimental values

As shown in Figure 8 (a), the material model developed through the TTSP shifting and curve fitting processes has a high accuracy in expressing the raw viscoelastic modulus response of the adhesive.

However, as shown in Figure 8 (b), compared to the modulus response in the DMA T_g test (Section 2.2.1), the predicted modulus decreases more slowly around the T_g. This could be due to the further curing of the exaimed adhesive sample during DMA multi-frequency scans test at high temperatures, which has received little attention in literatures. In real life applications, the adhesive may also have further curing at elevated ambient temperatures during the long-term service, which to some extent counteracts the effect of further curing of the sample in the accelerated chacatersing test. Further investigation of this issue was not possible within the current study, but nevertheless the comparison shown in here identifying the need for further research.

4 Numerical study of the behaviour of the FRP-to-steel joint

This section presents an FE analysis of an adhesive-bonded single lap-shear joint to investigate the effect of elevated temperatures on the behaviour of bonded joints in civil engineering applications. The constitutive material model developed in Section 3 was used to determine the time-temperature dependent viscoelasticity of the adhesive layer.

Three temperature levels were applied:

- 30 °C, being a slightly warmer temperature compared to the ambient condition;
- 40 °C, which is a potential elevated temperature in civil engineering conditions;
- 50 °C, which is consistent with the maximum operating temperature stipulated in current design guidelines, which should be a minimum of 15 °C below the peak Tan δ T_g, giving a 51.4 °C (66.4 °C - 15 °C) for the studied adhesive [7,23,24].

4.1 FE model for the adhesive-bonded single lap-shear joint

Figure 9 shows the geometry of the studied lap-shear joint, which was developed according to BS 5350-C5 [45].

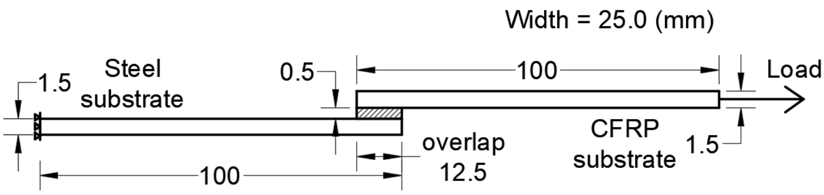

Figure 9: Geometry of the adhesive-bonded single lap-shear joint (dimensions in mm)

The joint was modelled in Abaqus using CPS4R planar stress elements with reduced integration and hourglass control to limit the stress singularity effect [44,46]. Finer meshes (0.1 mm) were applied to the area close to the overlap. The CFRP substrate was modelled as elastic with a Yong's modulus of 170 GPa and a Poisson's ratio of 0.3, while the steel substrate was modelled as elasto-plastic with a Young's modulus of 205 GPa, a yield strength of 355 MPa and a Poisson's ratio of 0.3. The adhesive layer was defined as viscoelastic material. The temperature was uniformly applied to all parts of the model. The load of 1 kN was applied to the CFRP substrate, which can result in a high instantaneous stress in the adhesive joint (but below the strength of the adhesive [32]) to investigate the behaviour of stress redistribution.

Note that this study focuses on the impact of viscoelastic creep of the structural adhesive on the response of the FRP-to-steel bonded joint. The joint damage related to the strength of the joint is not within the scope of this study, as a result, perfect bond was assumed between different sections.

4.2 The effect of viscoelasticity of the adhesive on the bonded joint

Figure 10 illustrates the creep compliances of the studied adhesive at elevated temperatures, which were obtained from a single cube element (C3D8) model, whilst it can also be calculated from equation (1) and (4).

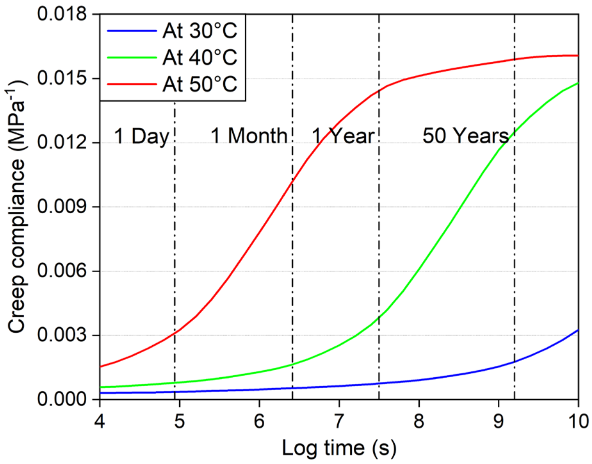

Figure 10: Creep compliances of the viscoelastic adhesive at various temperatures

The constitutive material model is sufficient to predict creep over the temperature range examined up to 50 years. After 50 years at 30 °C, the creep compliance of the adhesive increases almost as much as that after only 1 month at 40 °C, and even less than that after 1 day at 50 °C. Temperature has a great influence on the viscoelastic creep response of the adhesive, which will therefore affect the long-term behaviour of the adhesive bonded joint.

Figure 11 shows the effect of adhesive creep at 50 °C on the distribution of shear strain (LE12) and shear stress (S12) of the single lap-shear bonded joint. After 50 years (Figure 11 (b) and (d)), compared to the instantaneous behaviour of the joint (Figure 11 (a) and (c)), creep of the adhesive leads to a significant increase in the shear strain, however, it is accompanied by a redistribution behaviour of the shear stress, which reduces the concentrated shear stress at the edges of the joint and increases the effective stress transfer length.

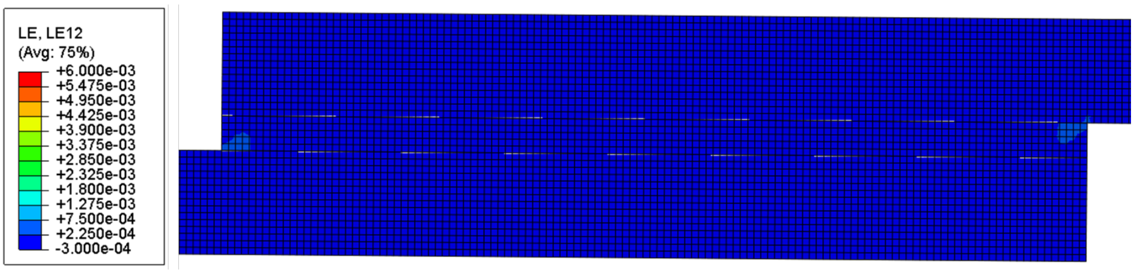

(a) instantaneous shear strain distribution after deformation

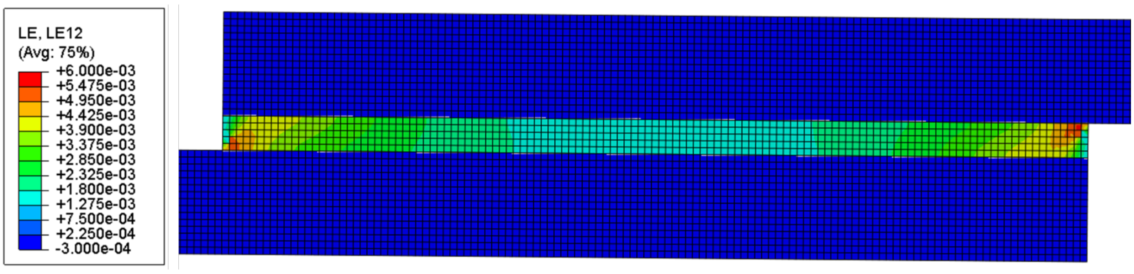

(b) shear strain redistribution after 50 years

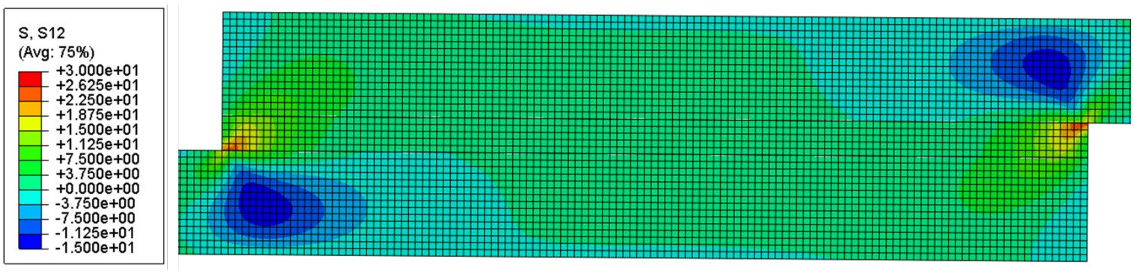

(c) instantaneous shear stress distribution after deformation

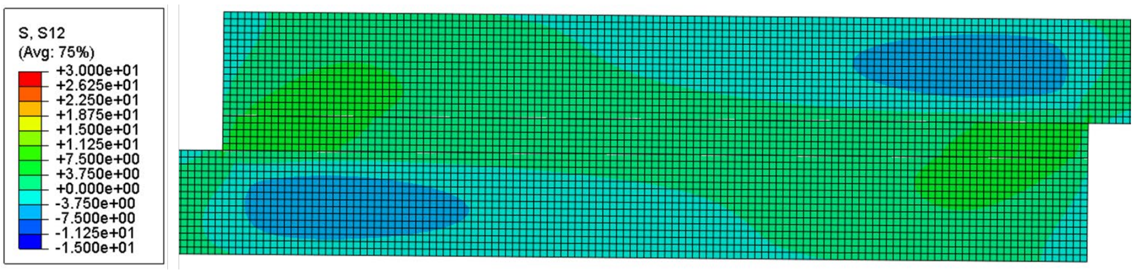

(d) shear stress redistribution after 50 years

Figure 11: Distribution of the shear strain and shear stress of the bonded joint at 50 °C

Figure 12 depicts the detailed changes in the maximum (concentrated) shear strain and shear stress at the edge of the joint over a period of 50 years at 30 °C, 40 °C, and 50 °C, respectively.

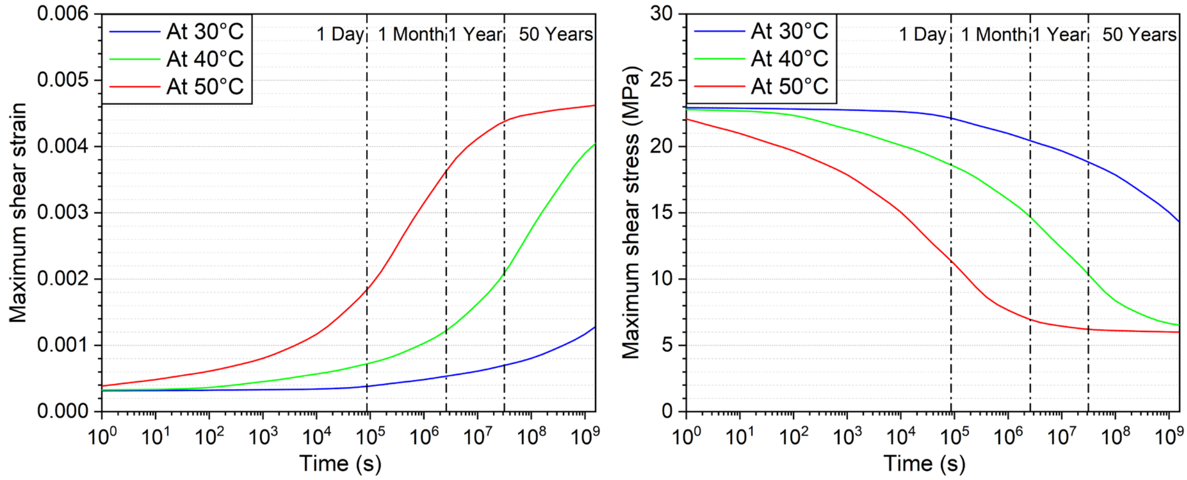

(a) maximum shear strain increasing with time (b) maximum shear stress decreasing with time

Figure 12: The shear strain and shear stress at the edge of the adhesive joint varying with time at different temperatures

At 30 °C, the maximum shear stress starts to decrease significantly after about 1 day due to the redistribution of stresses resulting from the viscoelastic behaviour of the adhesive layer. After 50 years, the maximum shear stress decreases by almost 37 % from about 23 MPa to 14.5 MPa, and the shear strain only increases by less than 0.001. This could be beneficial for the long-term performance of the bonded joint.

At 40 °C, the maximum shear stress begins to decrease within a few minutes, however, it is accompanied by a sharp rise in the rate of shear strain increase. Whilst the maximum shear stress decreases to about 6.5 MPa after 50 years, the maximum shear strain increased by more than three times compared to the results at 30 °C.

At 50 °C, the maximum shear stress and shear strain change significantly within the first year of use. This may indicate that the first year of service life of the bonded structure is critical under high operating temperature conditions, as creep in the joint may introduce significant shear strain, resulting in limited effectiveness of the bonded strengthening and the potential of early debonding failure.

5 Conclusions

In this study, a viscoelastic material model was developed for a typical structural epoxy adhesive (Sikadur®-330 [32]) by applying an accelerated test method involving dynamic mechanical analysis (DMA) and time-temperature superposition principle (TTSP), which was utilised to investigate the effects of elevated temperatures on the response of the adhesive-bonded FRP-to-steel joint.

The process of the accelerated tests has been illustrated and the limitations of applying this method have been discussed:

- The thermal stability of studied samples should be examined prior to performing DMA characterisation tests at high temperatures (> 100 °C).
- Materials that obey TTSP should be thermorheologically simple, which can be confirmed using the wicket plot.
- DMA tests may be challenging to characterise the nonlinear viscoelasticity of the sample, and the sample can be further cured in high temperature tests.

Whilst the accelerated test method has some limitations and requires further research, it remains a viable option for estimating the long-term behaviour of bonded joints, as it is impractical to carry out the conventional sustained load creep tests for decades to fully cover the design life of civil engineering structures.

The numerical study results of the single lap-shear FRP-to-steel joint indicate that:

- Elevated temperatures have a great influence on the creep response of the adhesive layer. The creep can lead to a significant increase in the shear strain of the adhesive joint accompanied by a redistribution behaviour of the shear stress, which reduces the concentrated shear stress at the edges of the joint and increases the effective stress transfer length.

- A slightly warmer temperature (30 °C for this study) than ambient environments is considered to be beneficial for the bonded joint as it can reduce the concentrated shear stress (by 37 % after 50 years) with negligible increase in the shear strain (by 0.001 after 50).
- However, higher temperatures (⩾40 ° C in this study) significantly increase the creep rate of the adhesive, resulting in a multifold increase in shear strain of the joint with limited reduction in the shear stress, which can be detrimental.

For cyclic (oscillating) temperature conditions, when the maximum temperature exceeds 40 °C, attention should also be paid to the detrimental effects of viscoelastic creep on bonded joints [47].

The available characterisation data and material models for adhesives used in civil engineering are limited. The developed viscoelastic model can be used for further numerical analysis as long as the applied adhesive is the same and has a similar T_g. For other structural adhesives, it will be necessary to carry out similar tests and modelling work (described in Section 2 and 3) to develop the corresponding material models.

The long-term creep failure of the joints tends to lead to interface fracture in FRP-strengthened structures, which has so far lacked satisfactory explanations and predictions. The constitutive material model developed in this paper focuses on analysing the viscoelasticity of the structural adhesive, whereas for the future study, the plasticity and the damage of the FRP-to-steel bonded joint will also be significant to investigate.

CRediT authorship contribution statement

S. Wang: Methodology, Formal analysis, Investigation, Writing - original draft, Visualization. **T. Stratford:** Conceptualization, Resources, Writing - review & editing. **T.P.S. Reynolds:** Writing - review & editing.

Declaration of competing interest

The authors declare that they have no known competing financial interests or personal relationships that could have appeared to influence the work reported in this paper.

Acknowledgments

The authors are grateful for the support from the International Collaborative Research Fund for Young Scholars in the Innovation Demonstration Base of Ecological Environment Geotechnical and Ecological Restoration of Rivers and Lakes. This work was funded by the Doctoral Research Starting Foundation of Hubei University of Technology under Grant [XJ2022001301].

References

[1] Karbhari VM, Shulley SB. Use of Composites for Rehabilitation of Steel Structures—Determination of Bond Durability. J Mater Civ Eng 1995;7:239–45. https://doi.org/10.1061/(asce)0899-1561(1995)7:4(239).

[2] Higgins A. Adhesive bonding of aircraft structures. Int J Adhes Adhes 2000;20:367–76. https://doi.org/10.1016/S0143-7496(00)00006-3.

[3] Heshmati M, Haghani R, Al-Emrani M. Environmental durability of adhesively bonded FRP/steel joints in civil engineering applications: State of the art. Compos Part B Eng 2015;81:259–75. https://doi.org/10.1016/j.compositesb.2015.07.014.

[4] Hollaway LC, Teng JG. Strengthening and Rehabilitation of Civil Infrastructures Using Fibre-Reinforced Polymer (FRP) Composites. Woodhead Publishing Ltd, UK; 2008.

[5] Heshmati M, Haghani R, Al-Emrani M. Durability of CFRP/steel joints under cyclic wet-dry and freeze-thaw conditions. Compos Part B Eng 2017;126:211–26. https://doi.org/10.1016/j.compositesb.2017.06.011.

[6] Ascione F, Granata L, Guadagno L, Naddeo C. Hygrothermal durability of epoxy adhesives used in civil structural applications. Compos Struct 2021;265:113591. https://doi.org/10.1016/j.compstruct.2021.113591.

[7] Cadei JMC, Stratford TJ, Hollaway LC, Dcukett WG. Strengthening metallic structures using externally bonded fibre-reinforced polymers. Construction Industry Research and Information Association (CIRIA), London, UK; 2004.

[8] Zhao XL, Zhang L. State-of-the-art review on FRP strengthened steel structures. Eng Struct 2007;29:1808–23. https://doi.org/10.1016/j.engstruct.2006.10.006.

[9] Zhao X-L. FRP-strengthened metallic structures. Taylor and Francis, Boca Rotan, FL; 2013.

[10] Heshmati M, Haghani R, Al-Emrani M. Durability of bonded FRP-to-steel jointsEffects of moisture, de-icing salt solution, temperature and FRP type. Compos Part B Eng 2017;119:153–67. https://doi.org/10.1016/j.compositesb.2017.03.049.

[11] He J, Xian G, Zhang YX. Numerical modelling of bond behaviour between steel and CFRP laminates with a ductile adhesive. Int J Adhes Adhes 2021;104:102753. https://doi.org/10.1016/j.ijadhadh.2020.102753.

[12] Ascione F, Granata L, Lombardi A. The influence of the hygrothermal aging on the strength and stiffness of adhesives used for civil engineering applications with pultruded profiles: an experimental and numerical investigation. J Adhes 2022;98:1733–1771. https://doi.org/10.1080/00218464.2021.1936507.

[13] Ascione F, Granata L, Carozzi G. Flexural and shear behaviour of adhesive connections for large scale GFRP frames: Influence of the bonded area and hygro-thermal aging. Compos Struct 2022;283:115122. https://doi.org/10.1016/j.compstruct.2021.115122.

[14] Teng JG, Yu T, Fernando D. Strengthening of steel structures with fiber-reinforced polymer composites. J Constr Steel Res 2012;78:131–43. https://doi.org/10.1016/j.jcsr.2012.06.011.

[15] Shishesaz M, Hosseini M. Effects of joint geometry and material on stress distribution, strength and failure of bonded composite joints: an overview. J Adhes 2020;96:1053–121. https://doi.org/10.1080/00218464.2018.1554483.

[16] Agha A, Abu-Farha F. Viscoelastic model to capture residual stresses in heat cured dissimilar adhesive bonded joints. Int J Adhes Adhes 2021;107:102844. https://doi.org/10.1016/j.ijadhadh.2021.102844.

[17] Feng CW, Keong CW, Hsueh YP, Wang YY, Sue HJ. Modeling of long-term creep behavior of structural epoxy adhesives. Int J Adhes Adhes 2005;25:427–36. https://doi.org/10.1016/j.ijadhadh.2004.11.009.

[18] Cree D, Gamaniouk T, Loong ML, Green MF. Tensile and Lap-Splice Shear Strength Properties of CFRP Composites at High Temperatures. J Compos Constr 2015;19:04014043. https://doi.org/10.1061/(asce)cc.1943-5614.0000508.

[19] de Zeeuw C, Teixeira de Freitas S, Zarouchas D, Schilling M, Lopes Fernandes R, Dolabella Portella P, et al. Creep behaviour of steel bonded joints under hygrothermal conditions. Int J Adhes Adhes 2019;91:54–63. https://doi.org/10.1016/j.ijadhadh.2019.03.002.

[20] Ke L, Li C, He J, Dong S, Chen C, Jiao Y. Effects of elevated temperatures on mechanical behavior of epoxy adhesives and CFRP-steel hybrid joints. Compos Struct 2020;235. https://doi.org/10.1016/j.compstruct.2019.111789.

[21] Shim W, Jang J, Choi JH, Cho JM, Yoon SJ, Choi CH, et al. Simulating rate- and temperature-dependent behaviors of adhesives using a nonlinear viscoelastic model. Mech Mater 2020;147:103446. https://doi.org/10.1016/j.mechmat.2020.103446.

[22] Zhang Y, Li W, Rui Y, Wang S, Zhu H, Yan Z. A modified cellular automaton model of pedestrian evacuation in a tunnel fire. Tunn Undergr Sp Technol 2022;130:104673. https://doi.org/10.1016/j.tust.2022.104673.

[23] National Research Council Advisory Committee. Guidelines for the design and construction of externally bonded FRP systems for strengthening existing structures - metallic structures. Rome, Italy: National Research Council; 2007.

[24] American Concrete Institute (ACI), Aci 440.2R-08: Guide for the design and construction of externally bonded FRP systems for strengthening concrete structures. USA; 2008.

[25] Houhou N, Benzarti K, Quiertant M, Chataigner S, Fléty A, Marty C. Analysis of the nonlinear creep behavior of concrete/FRP-bonded assemblies. J Adhes Sci Technol 2014;28:1345–66. https://doi.org/10.1080/01694243.2012.697387.

[26] Nguyen TC, Bai Y, Zhao XL, Al-Mahaidi R. Mechanical characterization of steel/CFRP double strap joints at elevated temperatures. Compos Struct 2011;93:1604–12. https://doi.org/10.1016/j.compstruct.2011.01.010.

[27] Sahin MU, Dawood M. Experimental Investigation of Bond between High-Modulus CFRP and Steel at Moderately Elevated Temperatures. J Compos Constr 2016;20:04016049. https://doi.org/10.1061/(asce)cc.1943-5614.0000702.

[28] Menard K, Menard N. Dynamic Mechanical Analysis, 3rd ed. CRC Press, Boca Rotan, FL, USK; 2020.

[29] Rouleau L, Deü JF, Legay A, Le Lay F. Application of Kramers-Kronig relations to time-temperature superposition for viscoelastic materials. Mech Mater 2013;65:66–75. https://doi.org/10.1016/j.mechmat.2013.06.001.

[30] Abouhamzeh M, Sinke J, Jansen KMB, Benedictus R. Kinetic and thermo-viscoelastic characterisation of the epoxy adhesive in GLARE. Compos Struct 2015;124:19–28. https://doi.org/10.1016/j.compstruct.2014.12.069.

[31] Wang S, Stratford T, Reynolds TPS. Linear creep of bonded FRP-strengthened metallic structures at warm service temperatures. Constr Build Mater 2021;283:122699. https://doi.org/10.1016/j.conbuildmat.2021.122699.

[32] SIKA. Sikadur®-330 Data Sheet. Sika Construction Chemicals; 2017.

[33] Chin J, Forster A, Clerici C, Hunston D. Characterization of ambient temperature cure epoxies used in adhesive anchor applications. J Adhes 2010;86:1041–67. https://doi.org/10.1080/00218464.2010.515494.

[34] Qin G, Na J, Mu W, Tan W, Yang J, Ren J. Effect of continuous high temperature exposure on the adhesive strength of epoxy adhesive, CFRP and adhesively bonded CFRP-aluminum alloy joints. Compos Part B Eng 2018;154:43–55. https://doi.org/10.1016/j.compositesb.2018.07.059.

[35] Hidalgo-Salazar MA, Correa JP. Mechanical and thermal properties of biocomposites from nonwoven industrial Fique fiber mats with Epoxy Resin and Linear Low Density Polyethylene. Results Phys 2018;8:461–7. https://doi.org/10.1016/j.rinp.2017.12.025.

[36] ISO E. 11358-1: 2014—Plastics—Thermogravimetry (TG) of Polymers—Part 1: General Principles. International

Organization of Standardization: Geneva, Switzerland; 2014.

[37] Del Prete I, Bilotta A, Bisby L, Nigro E. Elevated temperature response of RC beams strengthened with NSM FRP bars bonded with cementitious grout. Compos Struct 2021;258:113182. https://doi.org/10.1016/j.compstruct.2020.113182.

[38] British Standards Institutions. BSI Standards Publication Plastics — Determination of dynamic mechanical properties. BS ISO 6721:2019; 2019. https://doi.org/https://doi.org/10.3403/BSISO6721.

[39] Adams RD. Adhesive bonding : science, technology and applications. Boca Raton, FL : Cambridge: CRC Press ; 2005.

[40] Wang S, Stratford T, Reynolds TPS. A comparison of the influence of nonlinear and linear creep on the behaviour of FRP-bonded metallic beams at warm temperatures. Compos Struct 2022;281:115117. https://doi.org/10.1016/j.compstruct.2021.115117.

[41] Knapp G, Oreski G, Pinter G. Method to characterize the damping behavior of thin passively constrained layer laminates using dynamic mechanical analysis (DMA) in shear mode. Polym Test 2015;42:215–24. https://doi.org/10.1016/j.polymertesting.2015.01.011.

[42] Springer M, Bosco N. Linear viscoelastic characterization of electrically conductive adhesives used as interconnect in photovoltaic modules. Prog Photovoltaics Res Appl 2020;28:659–81. https://doi.org/10.1002/pip.3257.

[43] Barbero EJ. Finite element analysis of composite materials using AbaqusTM. CRC press; 2013.

[44] Abaqus. ABAQUS user's manual 6.14. ABAQUS Inc; 2014.

[45] British Standards Institutions. BSI. BS 5350-C5:2002 Methods of Test for Adhesives. Determination of Bond Strength in Longitudinal Shear for Rigid Adherends. 2002.

[46] Teng JG, Zhang JW, Smith ST. Interfacial stresses in reinforced concrete beams bonded with a soffit plate: A finite element study. Constr Build Mater 2002;16:1–14. https://doi.org/10.1016/S0950-0618(01)00029-0.

[47] Wang S, Stratford T, Reynolds TPS. Creep of an FRP-strengthened metallic beam under cyclic temperature and cyclic load. J Constr Steel Res 2022;196:107417. https://doi.org/10.1016/j.jcsr.2022.107417.